



RPMME

Homepage: <http://publisher.uthm.edu.my/periodicals/index.php/rpmme>
e-ISSN : 2773-4765

Finite Element Analysis Study of Titanium Hip Implant Using Abaqus Software

Muhamad Abdul Naim Zurhana¹, Rosli Asmawi^{1*}

¹Faculty of Mechanical and Manufacturing Engineering,
Universiti Tun Hussein Onn Malaysia, Batu Pahat, 86400, MALAYSIA

*Corresponding Author Designation

DOI: <https://doi.org/10.30880/rpmme.2023.04.02.049>

Received 01 July 2023; Accepted 01 November 2023; Available online 15 December 2023

Abstract: Total hip arthroplasty, also known as the hip implant, is used to replace damaged bone on the hip joint. The stem design is crucial since it will influence the performance of hip arthroplasty. This study uses the finite element method to simulate the effect of different implant geometry to investigate the stress distribution and displacement magnitude. The design of the implant was made with CAD software, while the femoral bone used a topography scan. This study assigned two types of titanium alloy, Ti-6Al-4V, and Ti-13Nb-13Zr, to the design. SolidWorks was used to create and assemble designs into the femur, while the Abaqus workbench was employed to analyse stability and stress distribution. The displacement and stress distribution of the design is conducted based on walking conditions. Based on the simulation, the hollow-typed design with Ti-6Al-4V material developed the lowest displacement magnitude, 0.7751 μm . Meanwhile, the original design with Ti-13Nb-13Zr produced the lowest stress distribution, 177.11 Pa. In conclusion, removing additional features to the implant improves the implant stability but produces more stress than the implant that keeps its geometry integrity. The choice of materials is also the factor that affects the displacement and stress distribution.

Keywords: Titanium, Hip Implant, Finite Element Method

1. Introduction

The hip joint is the joint between the head of the femur and the acetabulum of the pelvis [1]. Its primary role is to support the body's weight in static and dynamic [2]. The hip joints were crucial for maintaining balance and keeping the pelvic inclination angle. A common referral source of hip joint pain is the groin and anterior thigh [3]. Numerous factors can cause hip pain and failure of the hip joint, primarily due to arthritis or traumatic injury [4]. In modern surgery, total hip arthroplasty is a standard treatment for hip joint failure [5].

Total hip arthroplasty, referred to as total hip replacement, is widely acknowledged as one of the twentieth century's advancements in orthopaedics [6]. An artificial implant replaces a hip joint that has

*Corresponding author: roslias@uthm.edu.my

2023 UTHM Publisher. All rights reserved.

publisher.uthm.edu.my/periodicals/index.php/rpmme

deteriorated due to aging or trauma. Furthermore, total hip arthroplasty reduces and enhances patient discomfort in critical and long-term circumstances [7]. Usually, in the fabrication of hip implants, biomaterials are essential due to their biocompatible properties [5].

In this study, the objective was to simulate hip implants' stress distribution and displacement using the finite element method. Also, in this study, the concept of material removal is applied. The Computer-Aided Design (CAD) model is constructed using SolidWorks software and analysed using Abaqus software.

2. Methodology

2.1 Create a Design Model

SolidWorks was used to construct the hip implant model for this study. Grabcab provided a topology scan that generated the femur bone model. The models will be imported into the Abaqus program to analyse the stresses placed on the implant and its degree of displacement. Abaqus software was employed to specify the hip implant and the femoral bone material. Before beginning the simulation, several parameters must be assigned, including the component characteristics, the boundary condition, and the loads occurring on the implant and femur bone. The simulation data will be examined for validity and compared to earlier research. The primary goal of this investigation is to examine stress distribution and displacement acting on the implants.

In the original and hollow-typed design, the thickness, degree of rotation about the axis of the neck and head, and the length of the intramedullary stem are constant. The thickness of the implant is 15 to 8 mm, the neck and head placement angle around the axis is 135° , and the length of the stem is 120 mm. Ti-6Al-4V and Ti-13Nb-13Zr will be used to implement in both designs. Figure 1 and 2 shows the parameters of both designs.

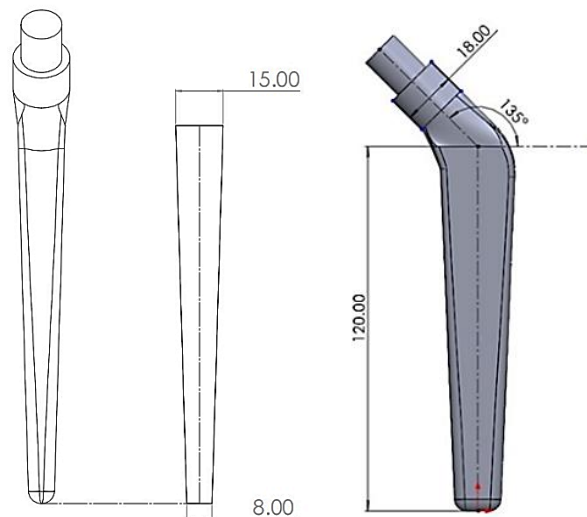


Figure 2: Parameters on hollow-typed implant

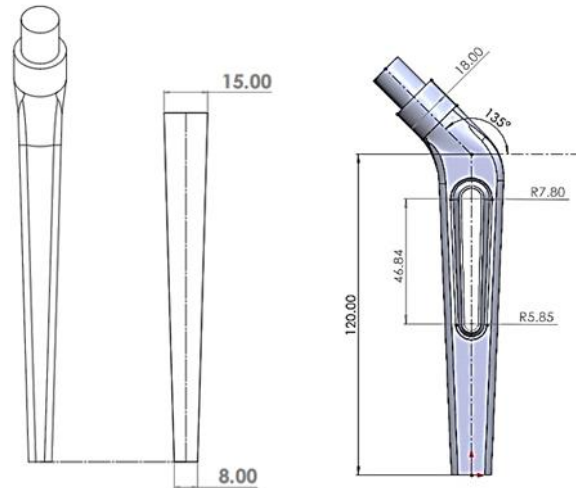


Figure 2: Parameters on hollow-typed implant

To design the hollow-typed implant, the radius on the upper side is 7.80 mm, and the radius on the lower side is 5.85 mm. The length between the upper and lower side is 46.84 mm.

2.2 Import the Model into Abaqus Software

After completing the design, both designs go through assembly in SolidWorks software to be merged into the femoral bone. Then the finished assembled models were saved in STEP format and imported into the Abaqus software. The STEP format was preferred as it contained more 3D data and part geometry than IGES. Thus, the Abaqus software can read the data designs.

2.2.1 Assign the Material Property

Before starting the simulation procedure, the implants were assigned based on mechanical properties in Table 1. The material of the implant chosen in this study is Ti-6Al-4V and Ti-13Nb-13Zr. The performances shown by Ti-6Al-4V and Ti-13Nb-13Zr are suitable for application in the human body because of their excellent biocompatibility [8], [9]. Table 1 shows the material properties of the human bone, Ti-6Al-4V, and Ti-13Nb-13Zr.

Table 1: Mechanical properties of human bone, Ti-6Al-4V, and Ti-13Nb-13Zr

Materials	Young's Modulus (GPa)	Poisson's Ratio (ν)
Human bone	17.3	0.3
Ti-6Al-4V	115	0.4
Ti-13Nb-13Zr	77	0.36

2.2.2 Topology Optimization

The topology process minimises the implant's unrelated features before proceeding to the meshing. Since the completed models were stored in SolidWorks' STEP format, extraneous features emerged on the implants. This process is essential to eliminate any unnecessary features that appear on the implant for a more precise meshing process.

2.2.3 Meshing of the Model

The meshing employed was linear tetrahedral mesh methods. The sophistication of the implant determines the mesh grid. The femur has a global mesh size of 4.5 mm for both experiments, while the

original design and hollow design have global mesh sizes of 1.25 mm and 1.955 mm, respectively. Figures 3 and 4 show the completed mesh of both models.



Figure 3: Completed mesh on the initial design

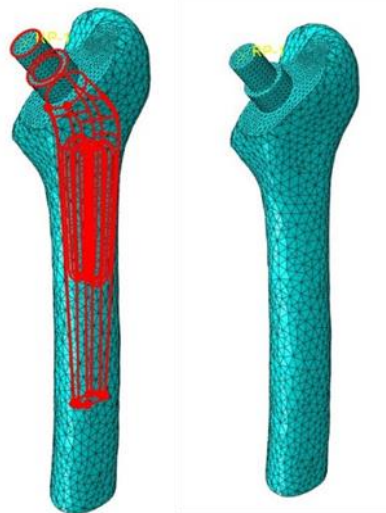


Figure 4: Completed mesh on the hollow design

2.2.4 Load and Boundary Conditions

The models are held in place by the boundary conditions set to the implant without any rotation operating on any axis, indicating that the models are static. The model's boundary conditions are ENCASTRE ($U1=U2=U3=UR1=UR2=UR3$), with all values set to 0. As illustrated in Figure 5, the weights were applied to the model at particular locations to mimic normal walking conditions. The amount of forces applied are referred from [10]. The value of forces is represented in Table 2.

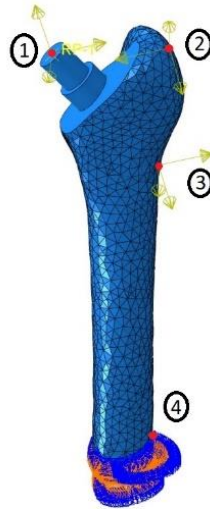


Figure 5: Locations of force being applied on the model

Table 2: Value of force for normal walking condition [10]

Point	X	Y	Z
1	433.8	263.8	-1841.3
2	-412.1	53.1	648.4
3	7.2	-148.6	-746.3
4	0	0	0

3. Results and Discussion

Results are acquired from the finite element method using Abaqus software. This study aims to identify the effect of material removal features and material selection on the stress distribution and displacement magnitude.

3.1 Relative Displacement

The range of relative displacement threshold values employed in this investigation was 40–150 μm . A value below 40 μm accelerates bone development to the implant site and encourages osteointegration. On the other hand, any value more than 150 μm will result in the development of a fibrous tissue membrane at the implant-femoral bone contact and hasten implant loosening [11]. Figure 6 and 7 below compares relative displacement for both implants and their material.

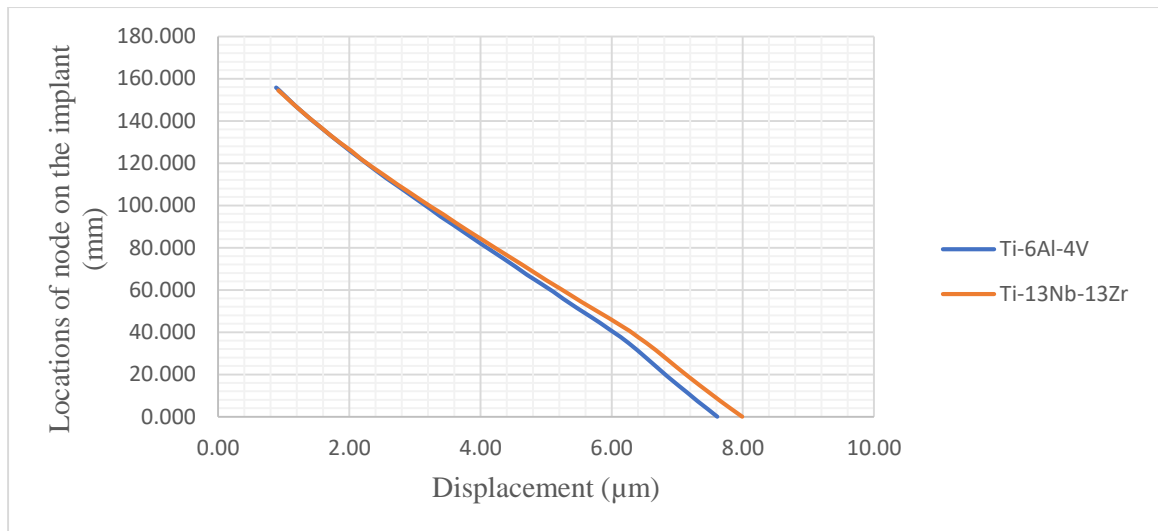


Figure 6: Graph of relative displacement on initial design

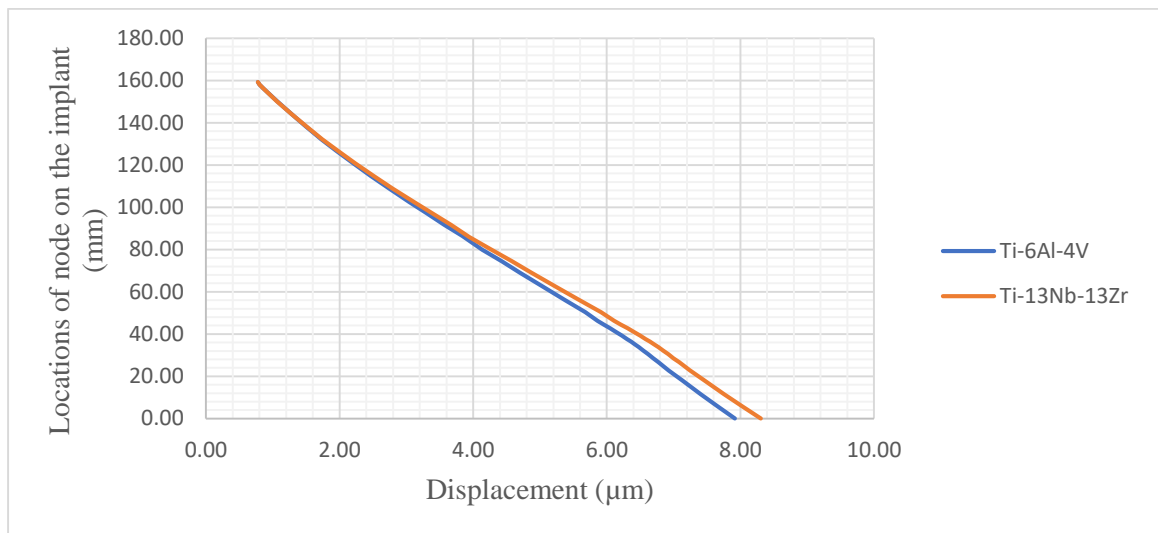


Figure 7: Graph of relative displacement on hollow design

From the graph above, the relative displacement of the hollow-typed design increases in comparison to the initial design. Ti-13Nb-13Zr achieved the lowest value in comparison with Ti-6Al-4V in the first design. For the initial design, the lowest relative displacement for Ti-13Nb-13Zr is 0.8792 μm , while Ti-6Al-4V is 0.8862 μm . Meanwhile, for the second design, the lowest relative displacement achieved by Ti-6Al-4V, the value is 0.7751 μm , while for Ti-13Nb-13Zr is 0.7754 μm . It concluded that both designs still do not exceed the threshold value of 40 μm . Thus, it can enhance the rate of bone growth to the implant surface.

3.2 Von Mises Stress

The stress distribution at the bone-implant contact is the main finding of this study. The amount of loading on the implant on the specified nodes is referred to as relative stresses. The stress distribution from the findings will be compared to the implant's material Young's Modulus to assess whether or not the different geometry will fail after adding loads. Figures 8 and 9 compare the stress distributions of both materials.

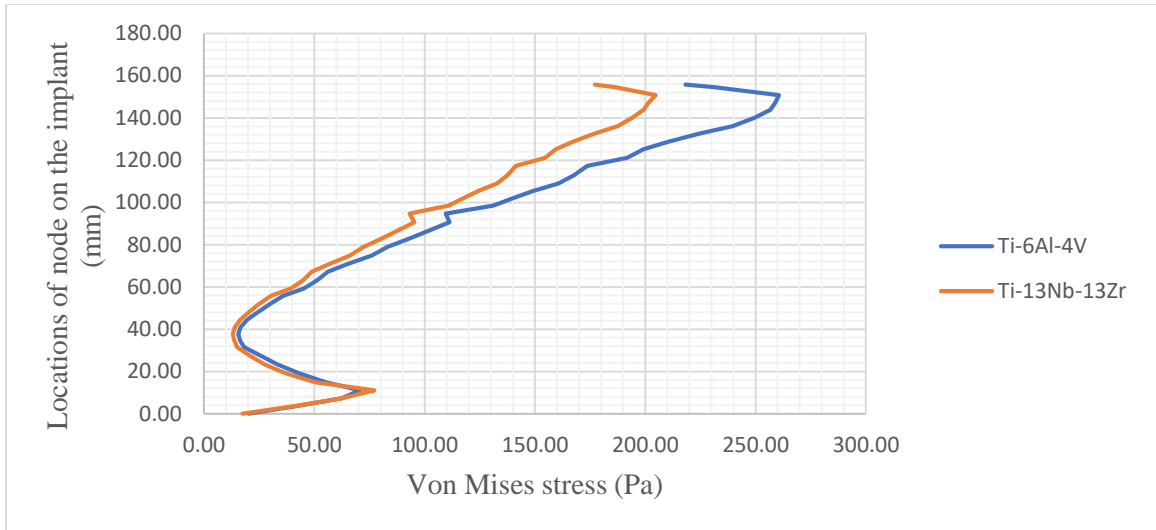


Figure 8: Graph of Von Mises stress on the initial design

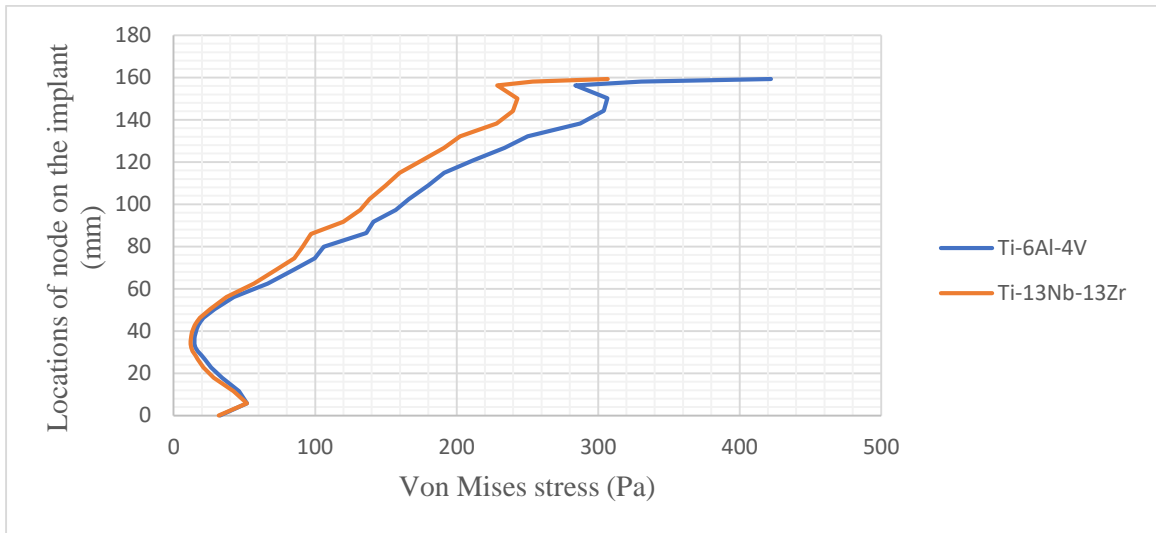


Figure 9: Graph of Von Mises stress on the second design

Results achieved by the hollow-type design produced a high value of Von Mises stress compared to the initial design. The highest value of stresses on the initial design of Ti-6Al-4V is 218.19 Pa, meanwhile, Ti-13Nb-13Zr is 177.11 Pa. The highest value of Ti-6Al-4V on the second design is 422.23 Pa and for Ti-13Nb-13Zr is 337.66 Pa. It can be observed that Von Mises stress occurred the lowest on the initial implant compared to the hollow design between these two materials.

4. Conclusion

The initial stability of the hip implant for total hip arthroplasty using the finite element methods was achieved by its relative displacement of the node on the implant surface to the node on the femur bone under walking conditions. The study's threshold value ranged from 40 to 150 μm . The relative displacement for Ti-6Al-4V achieved the lowest in the hollow-typed design. Meanwhile, for Ti-13Nb-13Zr, the material achieved the lowest in the initial design.

The highest value of stresses on the initial design of Ti-6Al-4V is 218.19 Pa. Meanwhile, Ti-13Nb-13Zr is 177.11 Pa. The highest value of Ti-6Al-4V on the second design is 422.23 Pa and for Ti-13Nb-13Zr is 337.66 Pa. It can be observed that Von Mises stress occurred the lowest on the initial implant compared to the hollow design between these two materials.

In conclusion, removing additional features to the implant improves the implant stability but produces more stress than the implant that keeps its geometry integrity. Also, the choice of materials is the factor that affects the displacement and stress distribution. Overall, the design with no hole feature is the best choice among the other options. The material of choice is Ti-13Nb-13Zr, as it has the lowest initial stability displacement and stress distribution.

Acknowledgement

The authors would like to thank the Faculty of Mechanical and Manufacturing Engineering, Universiti Tun Hussein Onn Malaysia for its support in this research.

References

- [1] D. P. Byrne, K. J. Mulhall, and J. F. Baker, "Anatomy & Biomechanics of the Hip," *Open Sport. Med. J.*, vol. 4, no. 1, pp. 51–57, 2014, doi: 10.2174/1874387001004010051.
- [2] A. Bedi, M. Dolan, M. Leunig, and B. T. Kelly, "Static and dynamic mechanical causes of hip pain," *Arthrosc. - J. Arthrosc. Relat. Surg.*, vol. 27, no. 2, pp. 235–251, 2011, doi: 10.1016/j.arthro.2010.07.022.
- [3] J. M. Leshner, P. Dreyfuss, N. Hager, M. Kaplan, and M. Furman, "Hip joint pain referral patterns: A descriptive study," *Pain Med.*, vol. 9, no. 1, pp. 22–25, 2008, doi: 10.1111/j.1526-4637.2006.00153.x.
- [4] N. J. Murphy, J. P. Eyles, and D. J. Hunter, "Hip Osteoarthritis: Etiopathogenesis and Implications for Management," *Adv. Ther.*, vol. 33, no. 11, pp. 1921–1946, 2016, doi: 10.1007/s12325-016-0409-3.
- [5] K. N. Chethan, Z. Mohammad, N. Shyamasunder Bhat, and B. Satish Shenoy, "Optimized trapezoidal-shaped hip implant for total hip arthroplasty using finite element analysis," *Cogent Eng.*, vol. 7, no. 1, 2020, doi: 10.1080/23311916.2020.1719575.
- [6] A. Fontalis, J. A. Epinette, M. Thaler, L. Zagra, V. Khanduja, and F. S. Haddad, "Advances and innovations in total hip arthroplasty," *Sicot-J*, vol. 7, 2021, doi: 10.1051/sicotj/2021025.
- [7] G. Kharmanda, "Integration of multi-objective structural optimization into cementless hip prosthesis design: Improved Austin-Moore model," *Comput. Methods Biomech. Biomed. Engin.*, vol. 19, no. 14, pp. 1557–1566, 2016, doi: 10.1080/10255842.2016.1170121.
- [8] M. Choroszyński, M. R. Choroszyński, and S. J. Skrzypek, "Biomaterials for hip implants - Important considerations relating to the choice of materials," *Bio-Algorithms and Med-Systems*, vol. 13, no. 3, pp. 133–145, 2017, doi: 10.1515/bams-2017-0017.
- [9] M. Geetha, A. K. Singh, R. Asokamani, and A. K. Gogia, "Ti based biomaterials, the ultimate choice for orthopaedic implants - A review," *Prog. Mater. Sci.*, vol. 54, no. 3, pp. 397–425, 2009, doi: 10.1016/j.pmatsci.2008.06.004.
- [10] M. Rafiq, A. Kadir, and U. N. Hansen, "the Effect of Physiological Load Configuration on Interface Micromotion in Cementless Femoral Stems," *Tissue Eng.*, no. 23, pp. 50–61, 2007.
- [11] N. Kohli, J. C. Stoddart, and R. J. van Arkel, "The limit of tolerable micromotion for implant osseointegration: a systematic review," *Sci. Rep.*, vol. 11, no. 1, pp. 1–11, 2021, doi: 10.1038/s41598-021-90142-5.